

Article

Identifying Sources and Assessing Potential Risk of Exposure to Heavy Metals and Hazardous Materials in Mining Areas: The Case Study of Panasqueira Mine (Central Portugal) as an Example

Carla Candeias ^{1,*}, Eduardo Ferreira da Silva ¹, Paula F. Ávila ² and João Paulo Teixeira ³

¹ GeoBioTec—Geobiosciences, Geotechnologies e Geoengineering Research Center, Geosciences Department, University of Aveiro, Campus de Santiago, Aveiro 3810-193, Portugal;

E-Mail: eafsilva@ua.pt

² LNEG—National Laboratory of Energy and Geology, Rua da Amieira, Apartado 1089, S. Mamede de Infesta 4466-901, Portugal; E-Mail: paula.avila@lneg.pt

³ Environmental Health Department, National Institute of Health, Rua Alexandre Herculano, 321, Porto 4000-055, Portugal; E-Mail: jpft12@gmail.com

* Author to whom correspondence should be addressed; E-Mail: candeias@ua.pt; Tel.: +351-968-337-915; Fax: +351-234-370-605.

External Editor: Jose A. Centeno

Received: 10 June 2014; in revised form: 15 September 2014 / Accepted: 17 September 2014 /

Published: 26 September 2014

Abstract: The Sn-W Panasqueira mine, in activity since the mid-1890s, is one of the most important economic deposits in the world. Arsenopyrite is the main mineral present as well as rejected waste sulphide. The long history is testified by the presence of a huge amount of tailings, which release considerable quantities of heavy metal(loid)s into the environment. This work assesses soil contamination and evaluates the ecological and human health risks due to exposure to hazardous materials. The metal assemblage identified in soil (Ag-As-Bi-Cd-Cu-W-Zn; potentially toxic elements (PTEs)) reflects the influence of the tailings, due to several agents including aerial dispersion. PTEs and pH display a positive correlation confirming that heavy metal mobility is directly related to pH and, therefore, affects their availability. The estimated contamination factor classified 92.6% of soil samples as moderately to ultra-highly polluted. The spatial distribution of the potential ecological risk index classified the topsoil as being of a very high ecological risk, consistent with wind direction. Non-carcinogenic hazard of topsoil, for children (1–6 years),

showed that for As the non-carcinogenic hazard represents a high health risk. The carcinogenic risks, both for children and adult alike, reveal a very high cancer risk mostly due to As ingestion.

Keywords: Panasqueira mine; potential toxic elements; modified contamination degree; non-carcinogenic hazard; carcinogenic risk; potential ecological risk factor and risk index

1. Introduction

Mine tailings, with considerable amounts of sulfides, left in the vicinity of environmentally sensitive locations, constitute one of the greatest threats to the surrounding environment. These materials when exposed to air and water are oxidized through chemical, electrochemical, and biological reactions, forming ferric hydroxides and sulfuric acid, leading to the generation of acid mine drainage with high contents of metals and sulfates, related to the alteration of sulfides, the equilibrium of which depends on their solubility [1–5].

Soil is prone to contamination both from hydrological and atmospheric sources. When soil is the receptor of tailings drainage, originating from metal mining and smelting, this waste disposal causes a major impact, and poses serious environmental concerns [6]. As a direct result of the mining activities, soil is generally, affected over a considerable area. The soil fine fraction is usually enriched in metals, due to the relative large surface area of fine particles that facilitate adsorption and metal binding to iron and manganese oxides and to organic matter [7,8]. Wind-blown dust originating from polluted soil is responsible for the aerial dispersion of trace metals [7]. Exposure to these hazardous elements may have different pathways, e.g., through the direct ingestion of soils and dust, ingestion of vegetables grown on contaminated soil or dust adhering to plants or dust inhalation. According to several authors [9–14] the studies dealing with the bioavailability and bioaccessibility of metal(loid) contaminants in highly-polluted soil are extremely useful to understand the possible effect on biota, and particularly on human health due to the exposure to these contaminants [12,15].

Among the purposes of environmental analysis are the determination of the geochemical background and natural concentrations of the chemical constituents in environment-background monitoring, as well as to determine the concentration of harmful pollutants in environment-pollution monitoring [16]. The sorption-desorption soil characteristics generally control the mobility and availability of heavy metals [17]. Heavy metal availability in soil depends on a number of factors, including Soil Organic Matter (SOM) and pH [18]. Soil pH plays the most important role in determining metal speciation, solubility from mineral surfaces, movement and bioavailability of metals [19–21]. Several laboratory experiments have shown that heavy metal mobility and availability have a negative correlation with pH [22]. Further, [23–25] documented that metal mobility and availability increases with the decrease of soil pH, thus enhancing the uptake of heavy metals by plants and, thereby, posing a threat to human health [26].

Exposure to increasing amounts of metal(loid)s in environmental and occupational settings is a reality worldwide, affecting a significant number of individuals. Most metal(loid)s are very toxic to living organisms and even those considered as essential can be toxic when in excess. They can disturb

important biochemical processes, constituting an important threat for human health. Major health effects include development retardation, endocrine disruption, kidney damage, immunological and neurological effects, and several types of cancer [27]. The identification of potential threats to human health and natural ecosystems is useful information [16]. The quantification of all the types of risks and the determination of the total risk of metal(loid)s to the exposed population through oral intake, inhalation and dermal contact [28] is also very important. Risk assessment is typically a multistep process of identifying, defining, and characterizing potentially adverse consequences of exposure to hazardous materials [28]. According to the Toxic Substances Portal [29], Ag, As, Cd, Cu, W and Zn are known to be toxic to humans, while arsenic and cadmium are classified as human carcinogens. Some studies also consider that Bi causes acute toxicity, and large doses can be fatal [30,31]. However, as Bi is considered to be one of the less toxic heavy metals, it is not included in this analysis.

In a previous paper from the same authors [32], several variables (Ag, As, Bi, Cd, Cu, W and Zn) showed moderate to strong correlation in the Panasqueira topsoil. This indicates an anthropogenic origin, especially linked to aerial transportation and deposition and/or to a geogenic origin. The main goals of the present study are: (a) establishment of the relationship between Potentially Toxic Elements (PTEs) with depth and soil pH; (b) assessment of soil contamination using a contamination factor for each pollutant; and (c) determination and evaluation of the ecological and human health risks due to exposure to hazardous materials.

2. Materials and Methods

2.1. Study Area

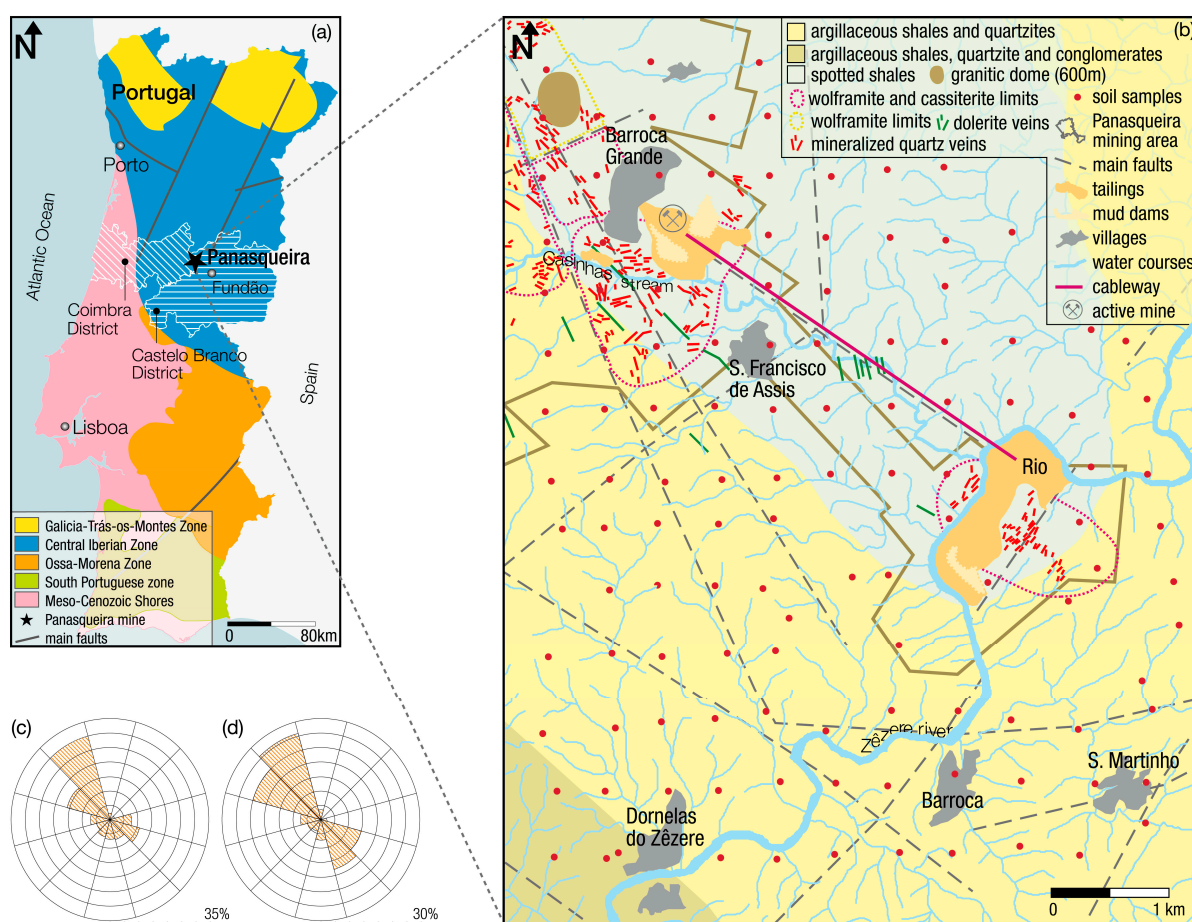
The active Panasqueira mine, exploited since the last decade of the 19th century, is located in Central Portugal (UTM (Universal Transverse Mercator) 29N, P 4445620.79, M 606697.31; Figure 1). It is considered to have the largest Sn-W deposit of Western Europe [33]. The geology has been extensively studied by many researchers [34–44]. Briefly, the Panasqueira deposit is a classic example of postmagmatic hydrothermal ore deposit, which is associated with Hercynian plutonism [36,41]. The paragenesis is complex with four stages of mineral formation identified: 1st stage, the oxide silicate phase (quartz, wolframite; cassiterite); 2nd phase, the main sulphide phase (pyrite, arsenopyrite, pyrrhotite, sphalerite, chalcopyrite); 3rd stage, the pyrrhotite alteration phase (marcasite, siderite, galena, Pb-Bi-Ag sulphosalts); and 4th stage, the late carbonate phase (dolomite, calcite) [38–49]. The Panasqueira deposit contains significant amounts of wolframite, arsenopyrite, chalcopyrite and cassiterite [34].

The long history of exploitation is testified by the presence of a huge amount of tailings and other debris (Figure 1b). The piles (Rio ~1.2 million m³; Barroca Grande ~7.0 million m³) and the mud dams (Rio ~0.7 million m³; Barroca Grande ~1.2 million m³) are exposed to atmospheric conditions, and are being altered by chemical, physical and geotechnical activities. On the top of the Rio tailings, an arsenopyrite stockpile (~9400 m³) was deposited and remained exposed until 2006 [41].

Topography ranges in altitude from 350 to 1080 m [47], with deep valleys of about 9%–25% inclination, constraining the soil into a very thin layer. Climate is severe, with dry and hot summers and very cold, rainy and windy winters. The annual precipitation ranges between 1200 and 1400 mm

with frequent snow falls, particularly above 700 m altitude. The mean annual temperature is 12 °C, ranging from 0 °C during the winter to 30 °C in the summer. The streams are generally dry in the summer and flooded in the winter. The prevailing wind in the area is NW-SE, with mean wind speeds of 4.22 m/s ($h = 10$ m), 5.55 m/s ($h = 40$ m) and 6.21 m/s ($h = 80$ m) (Figure 1c) [48–50]. The small villages around the mine have a historical dependence on soil and water use drinking water, agriculture, cattle rearing, fishing and forestry.

Figure 1. (a) Synthetic map of Portugal showing the location of Panasqueira mining area; (b) details of the study area, main geological units and soil samples grid - geological map adapted from [34,41,45]; (c) wind rose of the prevailing winds on the top of the mine (Barroca Grande tailing); and (d) on the top of a mountain 800 m north of the mine [46].



2.2. Field Sampling and Sample Preparation

Soil samples were collected according to a predefined grid (spaced ~400 m—Figure 1b). Two types of soil samples were collected at each sampling site: 122 topsoil (0–15 cm) samples and 116 subsoil samples collected below 15 cm depth. The difference in the total number of samples of each soil type is due to the presence at six sites of incipient and thin lithic soil derived from a substrate of metasediments. Topsoil samples were collected for the characterization of superficial contamination derived from the tailings, and subsoil samples to assess the extent of contamination at depth and simultaneously to identify geogenic markers. Approximately 50% of all samples were collected in duplicate. To establish

the local geochemical background, 47 unaffected soil samples (Bk) were also collected outside the contaminated area (Casegas area located NE, out of the influence of the Barroca Grande prevailing winds). The coordinates of each sample were determined by GPS and georeferenced with UTM (Universal Transverse Mercator) coordinates. All soil samples were collected after clearing the soil surface of superficial debris and vegetation, and placed in polyethylene bags. Samples were dried in a thermostatically controlled oven at 40 °C, disaggregated in a porcelain mortar, sieved (<2 mm), homogenized, split into aliquots and the analytical aliquot pulverized to <170 µm in a pre-cleaned mechanical agate mill for chemical analysis.

2.3. Chemical Analysis

Soil samples were submitted for multi-element analysis at the ACME Analytical Laboratories, which is an ISO 9002 Accredited Lab (Vancouver, Canada). A sample weight of 0.5 g was leached in hot (95 °C) aqua regia (HCl-HNO₃-H₂O), and concentrations were determined by Inductively Coupled Plasma Mass Spectrometry (ICP-MS) for Ag, As, Bi, Cd, Cu, W and Zn (detection limits of Ag, Bi, Cd, Cu, W < 0.1 mg·kg⁻¹; As < 0.5 mg·kg⁻¹; Zn < 1 mg·kg⁻¹).

Accuracy and analytical precision were determined using analytical results of certified reference materials (standards C3 and G-2) and duplicate samples in each analytical batch. The results were within the 95% confidence limits of the recommended values given for the certified materials. The Relative Standard Deviation (RSD) was between 5% and 10%.

Soil pH: numerous studies have verified that soil pH has a great effect on metal bioavailability [16,51,52]. The pH gives an indication of the acidity and alkalinity of soil. Many chemical reactions are pH dependent, and knowledge of the pH enables the prediction of the extent and speed of chemical reactions [53]. The procedure adopted for the determination of pH was modified from [54]. A suspension of soil was made up in five times its volume of a 0.01 mol/L solution of calcium chloride (CaCl₂) in water. The pH was measured using a calibrated pH-meter.

SOM: plays an important role in determining the fate of inorganic, as well as organic compounds in natural soil [55–58]. SOM can be roughly determined by measuring weight loss before and after ashing at 430 °C. Results are typically accurate to 1%–2% for soil with over 10% organic matter [53]. The procedure adopted was modified from [53]. Approximately 5 g of each sieved sample (<2 mm) was placed in a crucible and dried at 105 °C for 24 h. After cooling in a glass desiccator its weight was determined in a mass balance (resolution 0.001 g). The difference in weight gives the water content of each soil sample. The crucibles were then placed in a muffle furnace at 430 °C for 20 h. After cooling in a glass desiccator, the weight was measured on the same mass balance. The difference from the dry state gives the soil organic content (%).

2.4. Data Treatment of Data

Pearson's product-moment linear correlation coefficient matrix (r) was estimated in order to determine the extent of the relationship between the PTEs, pH and SOM [53]. The normality of statistical distribution of all data was verified by the Kolmogorov-Smirnov test ($\alpha = 0.05$) and Q-Q plots. The non-normal data were subjected to a non-parametric test or converted logarithmically to

ensure the validity of the results. The statistical analysis was performed using Six Sigma Statistica® (Stat Software Inc, Tulsa, OK, USA) and IBM® SPSS® Statistics software (IBM, New York, NY, USA).

Analysis of Variance (ANOVA) was carried out in order to assess the relationship between the Potentially Toxic Elements and the independent variables (depth, pH and SOM), by a two-way ANOVA test, according to the following expression:

$$Z_{ijk} = \mu + \alpha_i + \beta_j + \gamma_{ij} + \varepsilon_{ijk} \tag{1}$$

where, Z = the k th observation of the PTE taken at j th depth ($j = 1$ or 2) and i th soil property ($i = 1$ or 2), μ = the overall mean estimated, α = the depth effect, β = the soil property (pH or SOM), γ = the interaction between depth and the soil property, and ε = the residual error [59–61].

Log₁₀ transformation was applied to PTEs in order to convert the data to a normal or near-normal distribution and homogeneity of variances (Levene’s test, $p < 0.05$). For the two-way analysis of variance, samples were classified according to pH values (very acid (3.0, 4.0), acid (4.0, 6.0) and neutral (6.0, 7.0)) and SOM ((3.6, 10.0) and (10.0, 39.0) in %). It should be noted that the SOM classes established, were only defined for statistical purposes. In the cases where there were only two samples with neutral pH, this particular class was not considered further.

Contamination Factor and Modified Degree of Contamination was estimated using the method proposed by [62] in sediment pollution studies, but is also applied to soil studies [63,64]. It is based on the calculation, for each pollutant, of a contamination factor (CF_i) which is the ratio obtained by dividing the mean concentration of each metal in soil (C_i) by its corresponding baseline or background value (estimated from samples collected outside the area influenced by the mining activities) according to [65], and as explained in [6], *i.e.*, the background value, C_b (mg kg⁻¹), for the studied elements is as follows: Ag = 0.05; As = 22; Bi = 0.3; Cd = 0.01; Cu = 28; W = 0.35; Zn = 58) [64] (Table 1):

$$CF_i = C_i/C_b \tag{2}$$

Table 1. Classification and description of the Contamination factor (CF) [62] and the Modified contamination degree (mCd) [66].

CF Value	Level of the Contamination Factor	mCd Value	Modified Contamination Degree Gradations
$0 \leq CF < 1$	Low	$0 \leq mCd < 1.5$	None to very low
		$1.5 \leq mCd < 2$	Low
$1 \leq CF < 3$	Moderate	$2 \leq mCd < 4$	Moderate
$3 \leq CF < 6$	High	$4 \leq mCd < 8$	High
		$8 \leq mCd < 16$	Very high
		$16 \leq mCd < 32$	Extremely high
$6 \leq CF$	Very high	$32 \leq mCd$	Ultra high

In [66] is presented a modified and generalized form of the [62] equation for the calculation of the overall degree of contamination (mCd) for each sample as below:

$$mCd = \left(\sum_{i=1}^7 CF_i \right) / 7 \tag{3}$$

where CF_i is the contamination factor computed for each of the seven pollutants (Ag, As, Bi, Cd, Cu, W, Zn) considered in this study. In [66] is defined seven mCa degrees as shown in Table 1.

Potential ecological risk factor and risk index ($PERI$): is defined as the sum of the risk factors, which quantitatively defines the potential ecological risk of a contaminant in a sample, *i.e.*:

$$PERI_i = \sum_{i=1}^7 EF_i = \sum_{i=1}^7 CF_i \cdot TF \tag{4}$$

where $PERI_i$ is the Potential Ecological Risk Index for each sample (i); EF_i is the monomial potential ecological risk factor; CF_i is the single contamination factor (Equation (2)); and TF is the heavy metal toxic-response factor for each element. Soil toxic-response factors were computed for the seven selected elements according to the toxic factor requirements proposed by [62]. For this estimation there were used reference guide values of igneous rock types, soil, freshwater and land plants proposed by [67], and the land animals reference values proposed by [68]. The TF values obtained were: Zn = 1 < Cu = 2 < As = 5 < W = 15 < Bi = 20 < Cd = 30 < Ag = 35. In [62] are defined five EF classes and four $PERI$ degrees, as shown in Table 2.

Table 2. Monomial potential ecological risk factor (EF) and Potential ecological risk index ($PERI$) classification levels [62].

EF	Ecological Potential Risk for Single Substance	$PERI$	Ecological Risk
$0 \leq EF < 40$	Low	$PERI < 150$	Low
$40 \leq EF < 80$	Moderate	$150 \leq PERI < 300$	Moderate
$80 \leq EF < 160$	Considerable	$300 \leq PERI < 600$	Considerable
$160 \leq EF < 320$	High	$600 \leq PERI$	Very high
$320 \leq EF$	Very high		

Human health risk assessment calculations were based on the assumption that residents, both children and adults, are directly exposed to soil through three main pathways (a) ingestion; (b) dermal absorption and (c) inhalation of soil particles present in the air [69–72]. Ingestion of soil (i) occurs by eating soil particles and/or licking contact surfaces (e.g., hands). It is assumed that children present a higher ingestion rate, due to hand-to-mouth intake. Dermal absorption (ii) occurs through exposed skin, while soil is inhaled (iii) both by mouth and nose during breathing. Particles <10 μm (PM_{10}) are the more relevant in this process, although larger fractions of inhaled soil are, probably, decomposed in the gastrointestinal track. It is assumed that all contaminants are absorbed, both by the gastrointestinal tract or the lung [72]. Equations (5)–(7) were used to estimate the chronic daily intake of each exposure route considered [28,69,70,73], supplemented by specific quantitative information (Table 3):

$$CDI_{\text{ing}} = C_{\text{soil}} \times \frac{\text{IngR} \times EF \times ED}{BW \times AT} \times 10^{-6} \tag{5}$$

$$CDI_{\text{drm}} = C_{\text{soil}} \times \frac{SA \times SAF \times DA \times EF \times ED}{BW \times AT} \times 10^{-6} \tag{6}$$

$$CDI_{\text{inh}} = C_{\text{soil}} \times \frac{\text{InhR} \times EF \times ED}{PEF \times BW \times AT} \tag{7}$$

Table 3. Variables for estimation of soil residential risk in the Panasqueira mining area.

Parameters	Meaning	Values		Reference
		Child	Adult	
ABS_{gi}	fraction of contaminant absorbed in gastrointestinal tract	Ag 0.04; As 1.00; Cd 0.025; Cu 1.00; W 1.00; Zn 1.00		[28]
ABS_{drm}	fraction of contaminant absorbed dermally from soil	As 0.03; Cd 0.001		[28]
AT_c (d)	averaging time for carcinogenic effects	$LT \times 365$		[73]
AT_{nc} (d)	averaging time for non-carcinogenic effects	$ED \times 365$		[73]
BW (kg)	average body weight	15	70	[69,72]
C_{soil} (mg·kg ⁻¹)	concentration of the element in soil	-		
DA	dermal absorption factor	0.03 for As; 0.001 for other		[28]
CDI_{ing} (mg·kg ⁻¹ ·d ⁻¹)	chronic daily intake dose through ingestion	-		Equation (5)
CDI_{drm} (mg·kg ⁻¹ ·d ⁻¹)	chronic daily intake through dermal contact	-		Equation (6)
CDI_{inh} (mg·m ⁻³) (nc), (μg·m ⁻³) (c)	chronic daily intake through inhalation	-		Equation (7)
CSF_{ing} ((mg·kg ⁻¹ ·d ⁻¹) ⁻¹)	chronic oral slope factor	As 1.50		[28]
CSF_{drm}	chronic dermal slope factor	CSF_{ing}/ABS_{gi}		[28]
ED (yr)	exposure duration	6	24	[73]
EF (d·yr ⁻¹)	exposure frequency	350 residents		[73]
ET (h·d ⁻¹)	exposure time	24 residents		[73]
$IngR$ (mg·d ⁻¹)	soil ingestion rate	200	100	[73]
$InhR$ (m ³ ·d ⁻¹)	inhalation rate	7.6	20	[72]
IUR ((μg·m ⁻³) ⁻¹)	chronic inhalation slope factor	As 4.3×10^{-3} ; Cd 1.8×10^{-3}		[74]
LT (yr)	lifetime expected at birth	78 national		[75]
PEF (m ³ ·kg ⁻¹)	particle emission factor	1.36×10^9		[73]
SA (cm ²)	exposed skin area	2800	5700	[73]
SAF (mg·cm ⁻²)	skin adherence factor	0.2	0.07	[73]
RfD_{ing} (mg·kg ⁻¹ ·d ⁻¹)	chronic oral reference dose	Ag 5×10^{-3} ; As 3×10^{-4} ; Cd 1×10^{-3} ; Cu 4×10^{-2} ; Zn 0.3		[74]
RfD_{drm}	chronic dermal reference dose	$RfD_{ing} \times ABS_{gi}$		[28]
RfD_{inh} (mg·m ⁻³)	chronic inhalation reference dose	As 1.5×10^{-5} ; Cd 1×10^{-5}		[28]

The carcinogenic and non-carcinogenic side effects for each PTE were computed individually, as toxicity calculation uses different computational methods [76]. For each element and pathway, the non-cancer toxic risk was estimated by computing the Hazard Quotient (HQ , also known as non-cancer risk-Equation (8)) for systemic toxicity [73]. If HQ exceeds unity, it indicates that non-carcinogenic effects might occur. To estimate the overall developing hazard of non-carcinogenic effects, it is assumed that toxic risks have additive effects. Therefore, it is possible to calculate the cumulative non-carcinogenic hazard index (HI), which corresponds to the sum of HQ for each pathway (Equation (9)) [69,77]. Values of $HI < 1$ indicate that there is no significant risk of non-carcinogenic effects. While, values of $HI > 1$ imply that there is a probability of occurrence of non-carcinogenic effects, and are enhanced with increasing HI values [73]. The toxicity levels for each element were taken from The Risk Assessment

Information System (RAIS) [28]. The probability of an individual developing any type of cancer over a lifetime, as a result of exposure to the carcinogenic hazards, was computed for each pathway according to Equation (10) [78]. The carcinogenic risk was estimated by the sum of total cancer risk (Equation (11)). A cancer risk below 1×10^{-6} is considered insignificant. The result of 1×10^{-6} is classified as the carcinogenic target risk. If the cancer risk is above 1×10^{-4} it is qualified as unacceptable [69,79,80]:

$$HQ = \frac{CDI_{\text{pathway}}}{R_f D} \quad (8)$$

$$HI = \sum HQ = HQ_{\text{ing}} + HQ_{\text{drm}} + HQ_{\text{ihn}} \quad (9)$$

$$\text{Risk}_{\text{pathway}} = CDI_{\text{pathway}} \times CSF_{\text{pathway}} \quad (10)$$

$$\begin{aligned} \text{Risk} &= \sum \text{Risk}_{\text{pathway}} = \text{Risk}_{\text{ing}} + \text{Risk}_{\text{drm}} + \text{Risk}_{\text{ihn}} \\ &= CDI_{\text{ing}} \times CFS_{\text{ing}} + CDI_{\text{inh}} \times IUR + \frac{CDI_{\text{drm}} \times CSF_{\text{ing}}}{ABS_{\text{gi}}} \end{aligned} \quad (11)$$

Reference toxicity values were estimated as given in RAIS [28].

Spatial Estimation of extrapolated concentration values of chemical elements and contamination factors for the plotting of maps was based on geostatistics by extracting the necessary parameters for Ordinary Kriging from the variograms of each variable. Variograms were constructed and modelled with Surfer[®] (v. 8, Golden Software Inc, Golden, CO, USA), and the kriged estimations by Ordinary Kriging were also performed with Surfer[®].

3. Results and Discussion

3.1. Distribution of Ag, As, Bi, Cd, Cu, W and Zn in Soil Samples

Previous studies carried out in the Panasqueira area [6,43,44], allowed, through the topsoil concentrations, the characterization of the anthropogenic soil contamination due to the presence of tailings and open air impoundments.

Descriptive statistical parameters (median and range) for pH, SOM, Ag, As, Bi, Cd, Cu, W and Zn are summarized in Table 4. The individual element values are compared with the corresponding local geochemical background levels, and also with reference values from the literature.

All samples, both topsoil and subsoil, have a pH lower than 7. In particular, topsoil pH values range from 3.2 to 6.6; 35.9% of topsoil samples have pH values between 3.0 and 4.0; 59.2% are between 4.0 and 5.0; 4.2% from 5.0 to 6.0, and 1.7% from 6.0 to 7.0, *i.e.*, generally very acid to acid according to the United States Department of Agriculture classification [81]. As shown in Figure 2 (pH (a)), it is possible to identify that the areas with higher values are located around the villages Barroca Grande, S. Francisco de Assis, Rio, Barroca, Dornelas do Zêzere and S. Martinho. Around Rio and Barroca Grande tailings, the soil pH is above the 75th percentile (<4.1). The subsoil pH ranges from 3.6 to 6.2: 23.0% of the subsoil samples have pH values between 3.0 and 4.0; 73.5% are between 4.0 and 5.0; 2.7% from 5.0 to 6.0, and 0.9% from 6.0 to 7.0, *i.e.*, also generally very acid to acid. The highest pH value found in subsoil samples was located in Rio village (Figure 2 pH (b)) on the north section of the Rio tailings. In the surroundings of S. Francisco de Assis, Barroca Grande and Dornelas do Zêzere

villages, it is possible to identify some agricultural soil with $\text{pH} > 4.6$. Possibly these slightly higher pH values are due to land agricultural beneficiation techniques. Nevertheless, the soil of the present study area is overall classified as very acid to acid.

Figure 2. Spatial distribution of pH and soil organic matter (SOM, %) and Ag (mg kg^{-1}) for topsoil (a) and subsoil (b). Percentile class limits at P5, P10, P25, P50, P75, P90, P95 and P97.5. In blue are represented the main water courses, in grey the villages and in white the main tailings and dams. The green dashed lines represent the Ag background levels.

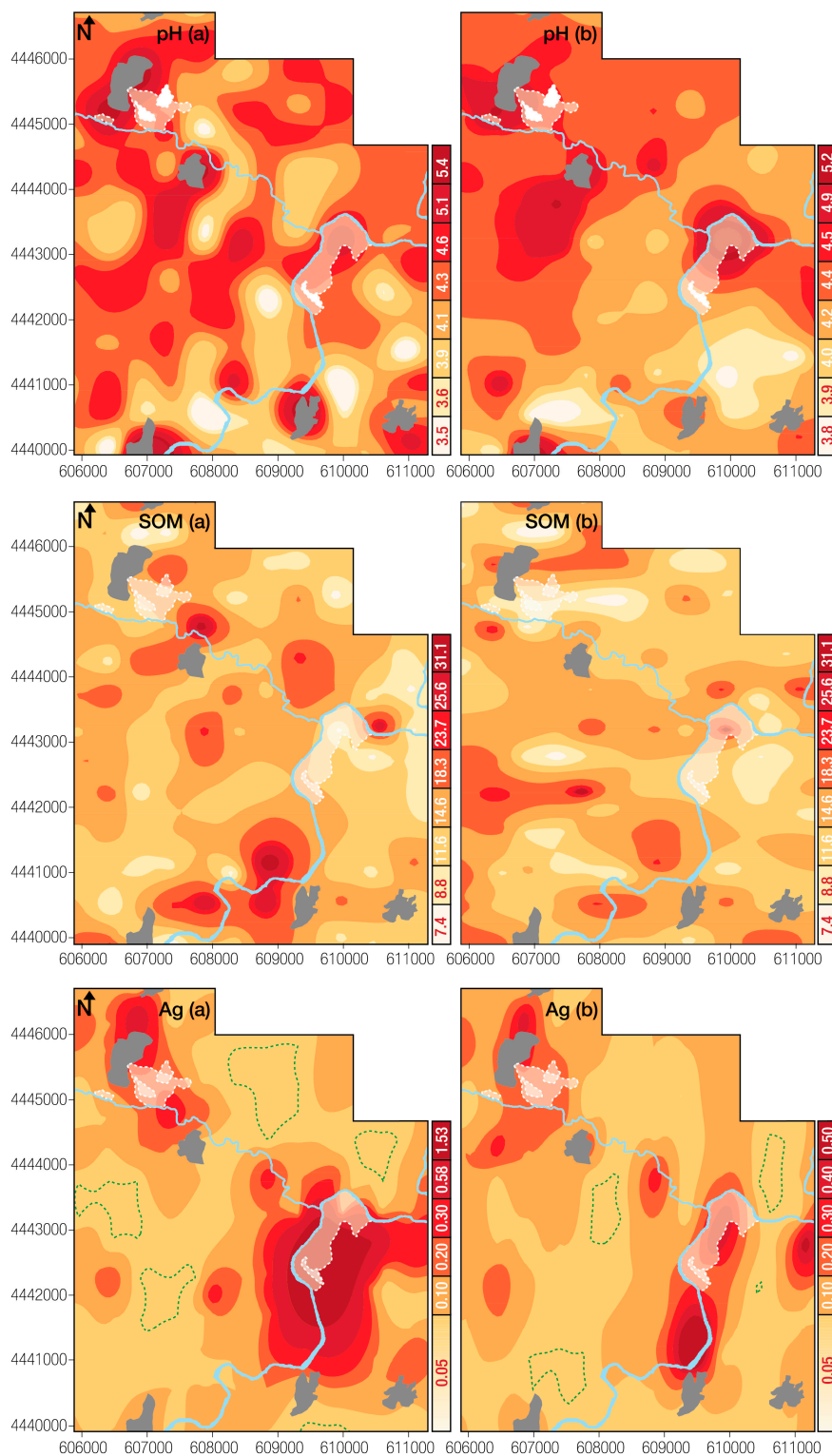


Table 4. Median, minimum and maximum concentrations values of topsoil and subsoil samples from Panasqueira mine and surrounding environment compared with international data. Casegas area, considered as representative of geochemical background (Bk).

Units		pH	SOM %	Ag mg·kg ⁻¹	As mg·kg ⁻¹	Bi mg·kg ⁻¹	Cd mg·kg ⁻¹	Cu mg·kg ⁻¹	W mg·kg ⁻¹	Zn mg·kg ⁻¹
Topsoil (n = 122)	Median	4.1	14.6	0.1	65	0.9	0.2	35	6	70
	Min–Max	3.2–6.6	5.7–39.0	0.05–1.7	17–1503	0.3–65	0.1–3	10–292	0.2–200	22–199
	Sk	1.59	1.2	4.72	6.98	9.21	3.77	4.80	5.40	1.38
Subsoil (n = 116)	Median	4.2	10.2	0.1	52	0.6	0.1	33	3	70
	Min–Max	3.6–6.2	3.6–19.5	0.1–0.6	8–350	0.2–15	0.1–1.5	12–146	0.1–29	16–192
	Sk	2.09	0.23	1.98	2.05	5.51	3.65	2.86	2.51	1.08
Geochemical background	Topsoil	4.2	14.5	0.1	63	0.8	0.20	34	4.4	68
	Subsoil	4.3	10.0	0.1	49	0.6	0.10	31	2.5	68
	Bk	3.98	10.5	0.05	22	0.3	0.01	28	0.4	58
Data from literature		6.0–8.0 ^a	1–20 ^b	0.07 ^c	11 ^d	0.3 ^c	0.1 ^d	16 ^d	1 ^d	55 ^d

Notes: SOM, soil organic matter; Sk, Skewness; Bk, background values, calculated according the [65] paradigm and confirmed by the [82] methods; ^a Ontario reference values [83]; ^b Normal Ranges in Soils [16,84,85]; ^c Mean World Soil [67,86]; ^d Median values for Portuguese Soil [87].

The topsoil SOM values range from 5.7% to 39.0% (see Table 4 and Figure 2 SOM (a)), while the subsoil SOM values vary from 3.6% to 19.5% (see Table 4 and Figure 2 SOM (b)). Comparing the topsoil and subsoil pH and SOM maps (Figure 2 and Table 4) is possible to observe that areas with the highest SOM values are related to areas with the lowest pH values.

To evaluate the presence of possible local anomalies the Ag (Figure 2), As, Bi, Cd (Figure 3), Cu, W, Zn (Figure 4) median and maximum values, observed in topsoil, were compared with the corresponding results in subsoil samples. Although the results tabulated in Table 4 show that Ag, As, Bi, Cu, W, and Zn present highest median and maximum values for topsoil when compared with subsoil, the paired samples *t*-test indicates that there are significant differences between soil samples at both depths for the elements As, Bi and W. Additionally, the results clearly show that there are higher contents in soil samples at both depths, when compared with the local geochemical background. The behavior of the topsoil element concentrations may reflect the influence of the Barroca Grande and Rio tailings and open air impoundments, possibly caused by aerial transport and deposition.

Topsoil samples, as shown in Table 5, have many strong to very strong correlation coefficients, *i.e.*, As/Ag, As/Bi, As, Cd, As/Cu, As/W, Ag/Bi, Ag/Cu, As/W, Bi/Cd, Bi/Cu, Bi/W, Cd/Cu, Cd/W, Cd/Zn, Cu/W. The strongest correlations are between Ag/Cu (0.94), As/Ag (0.90) and Bi/W (0.90). There is also a positive intermediate correlation ($r = 0.31$ to 0.70) between PTEs and pH. Several authors claim that heavy metal mobility holds a positive correlation with pH [18,88,89]. It is well known that pH affects heavy metal availability, since it is the major factor in controlling the ability of soil to retain heavy metals in an exchangeable form [21]. With low SOM the pH values may become relatively more important for the partitioning of metals. Most elements exhibit a weak negative correlation with SOM. For subsoil samples the PTEs correlation also presents some strong correlation coefficients (Table 5), but they are overall lower than in topsoil. The stronger correlations are between As/Bi ($r = 0.75$) and

Bi/Cu ($r = 0.69$). At this depth, pH is also the most significant soil property, presenting weak to intermediate positive correlations with the PTEs, except W.

Figure 3. Spatial distribution of As, Bi, Cd ($\text{mg}\cdot\text{kg}^{-1}$) values for topsoil (a) and subsoil (b). Percentile class limits at P5, P10, P25, P50, P75, P90, P95 and P97.5. The green dashed lines represent the elements background levels. In blue are represented the main water courses, in grey the villages and in white the main tailings and dams.

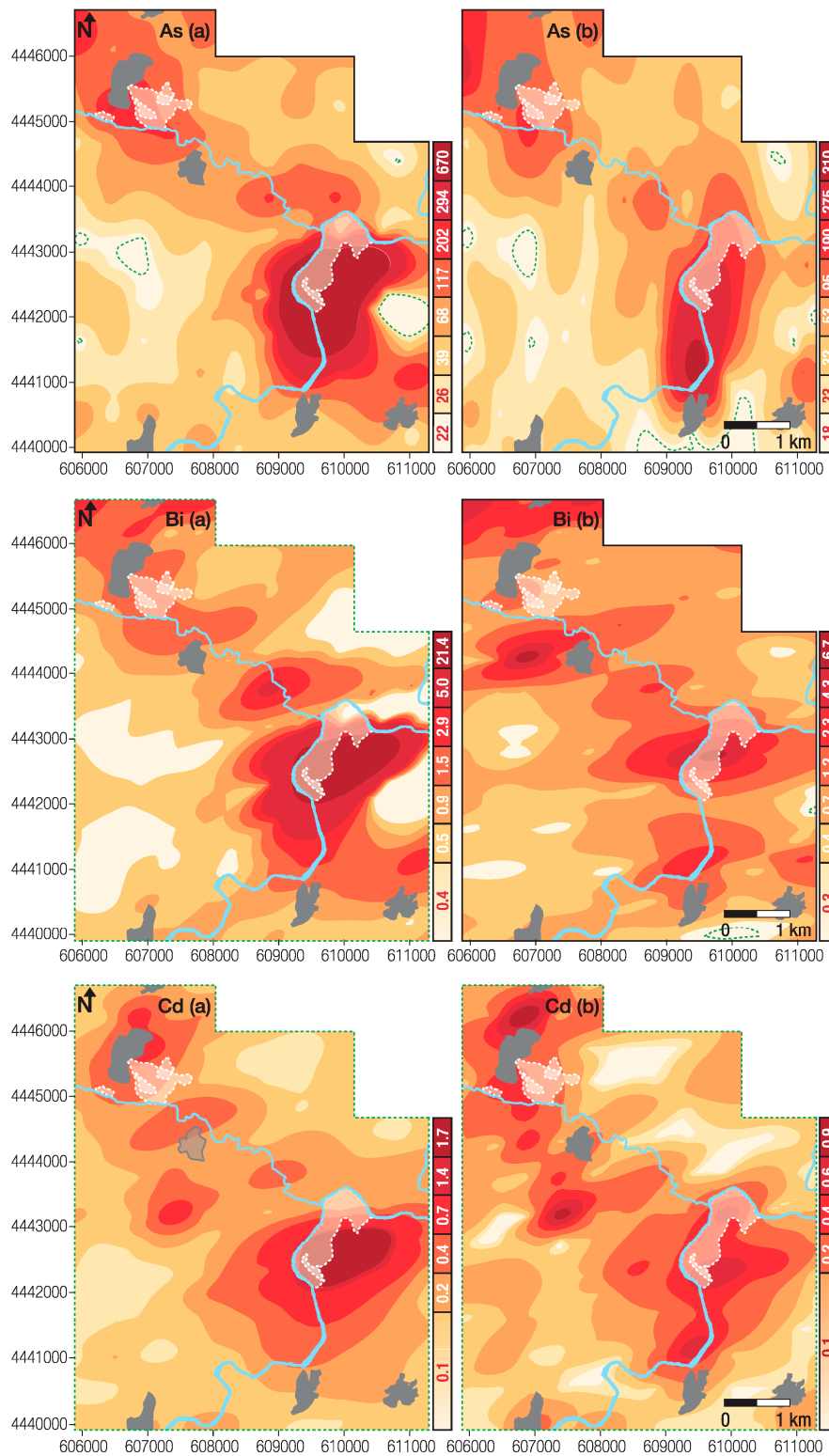


Figure 4. Spatial distribution of Cu, W, Zn ($\text{mg}\cdot\text{kg}^{-1}$) values for topsoil (a) and subsoil (b). Percentile class limits at P5, P10, P25, P50, P75, P90, P95 and P97.5. The green dashed lines represent the elements background levels. In blue are represented the main water courses, in grey the villages and in white the main tailings and dams.

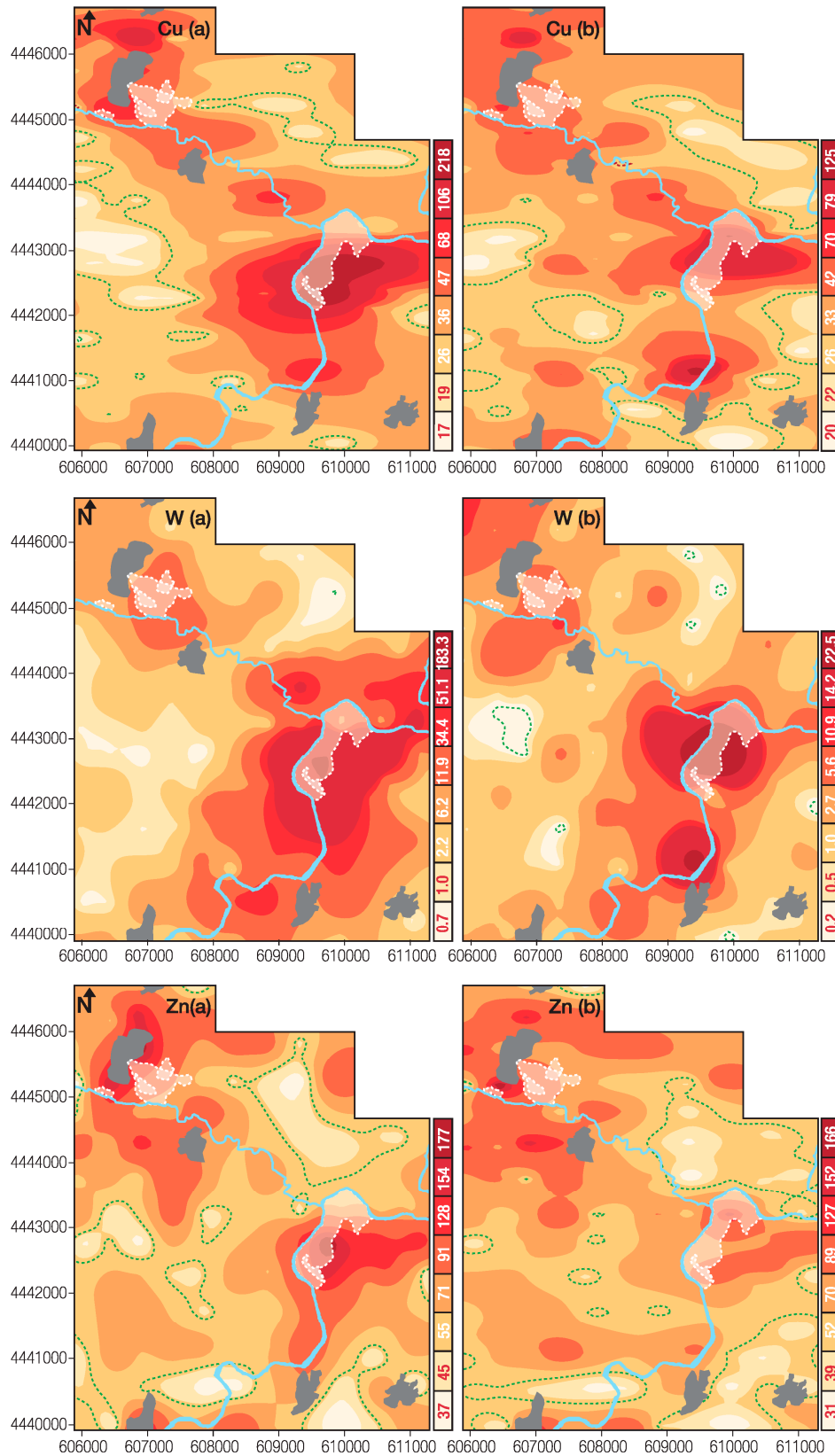


Table 5. Pearson's linear product-moment correlation coefficients for Ag, As, Bi, Cd, Cu, W, Zn, pH and SOM in topsoil ($n = 122$) and subsoil ($n = 116$) samples.

Var	Ag	As	Bi	Cd	Cu	W	Zn	pH	SOM	
Topsoil	Ag	1.00	0.90 **	0.84 **	0.79 **	0.94 **	0.83 **	0.51 **	0.70 **	-0.1
	As		1.00	0.84 **	0.77 **	0.89 **	0.81 **	0.44 **	0.37 **	-0.09
	Bi			1.00	0.82 **	0.87 **	0.90 **	0.44 **	0.54 **	-0.14
	Cd				1.00	0.86 **	0.79 **	0.68 **	0.42 **	-0.07
	Cu					1.00	0.80 **	0.60 **	0.61 **	-0.14
	W						1.00	0.38 **	0.46 **	0.01
	Zn							1.00	0.31 **	-0.15
	pH								1.00	-0.40 **
	SOM									1.00
Subsoil	Ag	1.00	0.43 **	0.34 **	0.45 **	0.42 **	0.36 **	0.43 **	0.30 **	0.15
	As		1.00	0.75 **	0.43 **	0.59 **	0.49 **	0.30 **	0.09	-0.01
	Bi			1.00	0.50 **	0.69 **	0.56 **	0.35 **	0.04	-0.01
	Cd				1.00	0.53 **	0.43 **	0.57 **	0.17	-0.09
	Cu					1.00	0.44 **	0.56 **	0.11	-0.17
	W						1.00	0.14	-0.21 *	0.16
	Zn							1.00	0.45 **	-0.23 *
	pH								1.00	-0.35 *
	SOM									1.00

Notes: ** Correlation is significant at the 0.01 level (2-tailed); * Correlation is significant at the 0.05 level (2-tailed).

In order to identify the most important factor controlling the different PTEs spatial differences concentrations, a two-way ANOVA was performed [90]. In this study, two models were selected to group the variables, (a) depth-SOM and (b) depth-pH. The results of the test between dependent (PTEs) and independent (depth and SOM) variables (Table 6) showed that soil depth accounts for significant variations between the group means: Bi ($p = 0.035$), Cd ($p = 0.015$) and W ($p = 0.009$). The independent variable SOM shows significant variations in the concentration of As ($p = 0.021$), Bi ($p = 0.068$), W ($p = 0.013$) and Zn ($p = 0.021$). There is no significant interaction between depth and SOM. While the independent variable pH (Table 7) shows that there are significant variations with depth for most PTEs (Ag $p = 0.071$; As $p = 0.027$; Bi $p = 0.001$; Cd $p < 0.000$; W $p < 0.000$), except for Cu ($p = 0.371$). pH presents a significant variation for Ag ($p = 0.031$), W ($p = 0.001$) and Zn ($p < 0.001$). The interaction between pH*depth shows no significant variations ($p > 0.050$), except on the concentration of Cu ($p = 0.038$).

3.2. Quantitative Assessment of Soil Contamination

In this study, a simplified approach to assess soil contamination based on comparing the measured concentrations in the Panasqueira soil with the geochemical background values for Casegas was adopted. Table 8 shows the results of contamination factors (CF) and the modified degree of contamination (mCd) for the selected elements in topsoil and subsoil, and also in Casegas soil.

Table 6. Two-way ANOVA results between the dependent (PTEs) and independent (depth, SOM) variables. PTEs were subjected to log-normal transformation (As, As, Cd, Cu, W and Zn with $\alpha = 0.050$; Bi with $\alpha = 0.075$).

Source of Variation	Dependent Variables	df	Mean Square	F	p-Value
Depth	Ag	1	0.223	1.624	0.204
	As	1	0.127	1.652	0.200
	Bi	1	0.333	4.484	0.035
	Cd	1	0.926	5.951	0.015
	Cu	1	0.012	0.483	0.488
	W	1	1.486	6.928	0.009
	Zn	1	0.062	1.933	0.166
SOM	Ag	1	0.010	0.076	0.783
	As	1	0.417	5.422	0.021
	Bi	1	0.251	3.371	0.068
	Cd	1	0.160	1.029	0.311
	Cu	1	0.007	0.275	0.601
	W	1	1.763	8.219	0.005
	Zn	1	0.173	5.372	0.021
Depth*SOM	Ag	1	0.051	0.373	0.542
	As	1	0.007	0.093	0.760
	Bi	1	0.001	0.008	0.928
	Cd	1	0.001	0.006	0.940
	Cu	1	0.037	1.52	0.219
	W	1	0.095	0.44	0.506
	Zn	1	0.002	0.06	0.811
Error	Ag	238	0.137	-	-
	As	215	0.077	-	-
	Bi	225	0.074	-	-
	Cd	233	0.156	-	-
	Cu	218	0.024	-	-
	W	215	0.215	-	-
	Zn	235	0.032	-	-

According to the topsoil median values of the contamination factor, Bi, Cd and W present an extremely high degree of contamination, while Ag and As a high contamination factor. The results demonstrated that mC_d values vary from the minimum 1.2 in both topsoil and subsoil to the maximum of 150 in topsoil, with median values varying from 4 in subsoil to 6 in topsoil. The cumulative frequency distribution indicates that only 7.4% of the soil samples were classified as no to low degree of pollution, with mC_d values < 2.0 , and the remaining soil samples (92.6%) registered moderate to ultra-high degree of pollution, with mC_d values equal or greater than 2.0 (27.9% between $2 \leq mC_d < 4$; 27.1% between $4 \leq mC_d < 8$; 19.7% between $8 \leq mC_d < 16$; 15.6% between $16 \leq mC_d < 32$ and 2.5% between $32 \leq mC_d$). The enrichment is more pronounced in topsoil (subsoil mC_d values ranged 1.2–26.4).

Table 7. Two-way ANOVA results between the dependent (PTEs) and independent (depth, pH) variables. PTEs were subjected to log-normal transformation (As, Bi, Cd, Cu, W, Zn with $\alpha = 0.050$; Ag with $\alpha = 0.075$).

Source of Variation	Dependent Variables	df	Mean Square	F	p-Value
Depth	Ag	1	0.353	3.296	0.071
	As	1	0.512	4.930	0.027
	Bi	1	0.832	10.605	0.001
	Cd	1	1.810	13.449	0.000
	Cu	1	0.019	0.805	0.371
	W	1	3.055	14.560	0.000
	Zn	1	0.007	0.266	0.607
pH	Ag	1	0.506	4.726	0.031
	As	1	0.031	0.301	0.584
	Bi	1	0.017	0.222	0.638
	Cd	1	0.020	0.146	0.703
	Cu	1	0.000	0.001	0.971
	W	1	2.315	11.033	0.001
	Zn	2	0.605	21.777	0.000
Depth*pH	Ag	1	0.116	1.085	0.299
	As	1	0.053	0.510	0.476
	Bi	1	0.082	1.040	0.309
	Cd	1	0.179	1.332	0.250
	Cu	1	0.104	4.351	0.038
	W	1	0.321	1.532	0.217
	Zn	2	0.077	2.769	0.065
Error	Ag	233	0.107	-	-
	As	230	0.104	-	-
	Bi	225	0.078	-	-
	Cd	226	0.135	-	-
	Cu	217	0.024	-	-
	W	213	0.210	-	-
	Zn	233	0.028	-	-

Table 8. Contamination Factors (CF) and Modified Degree of Contamination (mC_d) using geochemical background values. Casegas area is considered as representative of geochemical background.

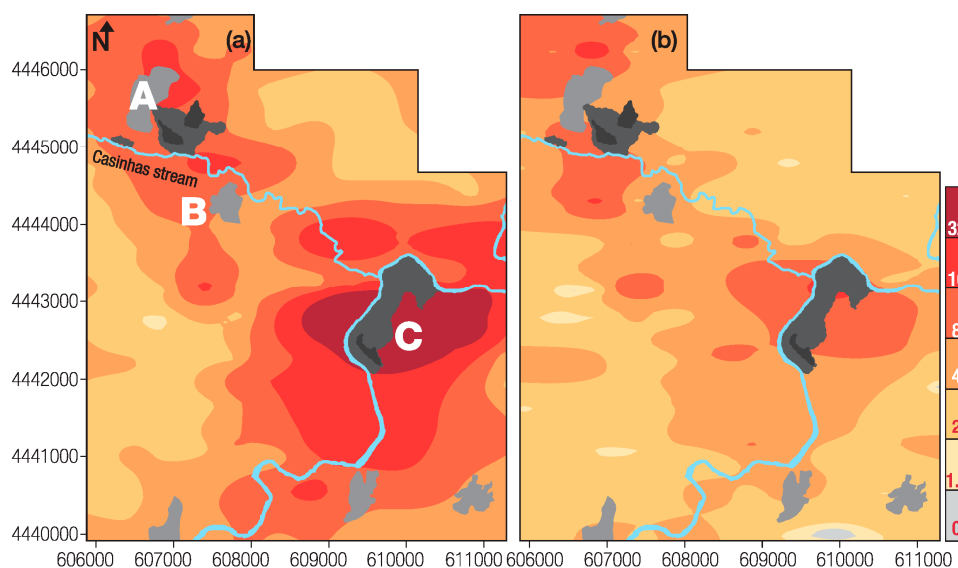
Var		Ag _{CF}	As _{CF}	Bi _{CF}	Cd _{CF}	Cu _{CF}	W _{CF}	Zn _{CF}	mC _d
Bk	Min	1.0	0.4	0.7	1.0	0.6	0.1	0.3	0.7
	Med	1.0	1.0	1.0	1.0	1.0	1.1	1.0	1.4
	Max	8	5	9	30	6	26	2	13
Topsoil	Min	1.0	0.8	1.0	5.0	0.4	0.6	0.4	1.2
	Med	2	3	3	20	1.2	17	1.2	6
	Max	34	68	215	300	10	571	3	150
Subsoil	Min	1.0	0.4	0.7	5.0	0.4	0.1	0.3	1.2
	Med	2	2	2	10	1.1	8	1.2	4
	Max	12	16	51	150	5	84	3	26

Casegas is considered as an uncontaminated site, since it is outside the mine area and the influence of airborne polluted dust. The maximum mC_d value of 13.1, represents a very high contamination degree, which is mostly due to the Cd and W contamination factors. In this case, however, the high mC_d value is most likely due to geogenic sources, as this is a naturally enriched and mineralized zone.

The calculated mC_d values make possible the assessment of the spatial distribution of the modified degree of contamination. The first step is the determination of the spatial structure of the new variables, and the experimental variograms were used to model the data using exponential models, the extracted parameters are for topsoil: main direction = 90°; Nugget effect (C_0) = 30; Sill-Nugget effect (C_1) = 330; range of influence (length) = 1200 m; anisotropy ratio = 1.81; and for subsoil: main direction = 90°; C_0 = 0; C_1 = 19; length = 900 m; anisotropy ratio = 2.90. Estimation of the spatial distribution was then achieved by Ordinary Kriging and the respective map plotted. In Figure 5 it is possible to observe the mC_d spatial distribution revealing areas with very high values.

Figure 5 shows that soil samples collected near the Barroca Grande tailings (A), Rio tailings (C) and the mud impoundments stand out clearly, because the soil is enriched in Ag, As, Bi, Cd, Cu, W and Zn; all soil samples from both depths taken from Barroca Grande exceed the As, Bi, Cd and W baseline values for Portugal, while at Rio only Zn in some samples (25%) has concentrations that are lower than the guide value. According to [42], the Barroca Grande tailings and open impoundments have high As, Cd, Cu, Pb, W, and Zn concentrations (mean content in the more coarse tailings material As = 7142 mg·kg⁻¹; Cd = 56 mg·kg⁻¹; Cu = 2501 mg·kg⁻¹; Pb = 172 mg·kg⁻¹; Sn = 679 mg·kg⁻¹; W = 5400 mg·kg⁻¹ and Zn = 1689 mg·kg⁻¹ and mean content in the impoundment material (rejected from the mill operations) As = 44,252 mg·kg⁻¹; Cd = 491 mg·kg⁻¹; Cu = 4029 mg·kg⁻¹; Pb = 166 mg·kg⁻¹; Sn = 454 mg·kg⁻¹; W = 3380 mg·kg⁻¹ and Zn = 3738 mg·kg⁻¹). The mineralogy of these tailings consists of mainly quartz, muscovite, kaolinite, illite-montmorillonite, montmorillonite-vermiculite, and chlorite, and also arsenopyrite, wolframite, and natrojarosite.

Figure 5. Spatial distribution of the modified degree of Contamination (mC_d) for topsoil (a) and subsoil (b). Values were estimated on the basis of the concentration factors of Ag, As, Bi, Cd, Cu, W and Zn (A, Barroca Grande; B, S. Francisco de Assis; C, Rio).



The dams at Barroca Grande may pose a significant potential threat, due to the fine-grained nature of the materials, and their location with respect to the Casinhas stream that cross S. Francisco de Assis village. The X-Ray Diffraction (XRD) analysis of the impoundment material revealed the presence of scorodite, arsenopyrite, quartz, sphalerite, hematite, and muscovite. These tailings and impoundment material are metal-enriched at such a level, likely to be toxic to the ecosystem [42]. The concentrations exceed the values defined for the 90th percentile of the South Portuguese Zone (As $157 \text{ mg}\cdot\text{kg}^{-1}$; Cu $108 \text{ mg}\cdot\text{kg}^{-1}$; Ni $62 \text{ mg}\cdot\text{kg}^{-1}$; Pb $117 \text{ mg}\cdot\text{kg}^{-1}$; Zn $134 \text{ mg}\cdot\text{kg}^{-1}$), which is indicative of enrichment in trace metals. This Ag-As-Bi-Cd-Cu-W-Zn association is quite logical and is linked to the Panasqueira ore-paragenetic association. The highest mC_d values identified near Barroca Grande (A), São Francisco de Assis (B) and Rio (C) confirms that mechanical and chemical dispersion from Barroca Grande and Rio tailings and mud impoundments occurs. Most of the samples (90% or higher of total samples) collected from Barroca Grande (A), São Francisco de Assis (B) and Rio (C) villages, exhibit mC_d values >8.0 , clearly indicting a very high degree of contamination.

The Panasqueira tailings impoundments have been and are affected by surface water flows (from heavy rainfall events) that have eroded the tailings from their original location and transported the materials downstream to residential areas (namely to S. Francisco de Assis). However, the superficial flat of the tailings have dried and are susceptible to wind erosion. The relative rates of water and wind erosion and transport, in Barroca Grande, São Francisco de Assis and Rio, suggest that wind processes have similar, and in many cases greater, impact on loss and local redistribution of soil in ecosystems than an eventual erosional soil enrichment.

3.3. Potential Ecological Risk Factor and Risk Index

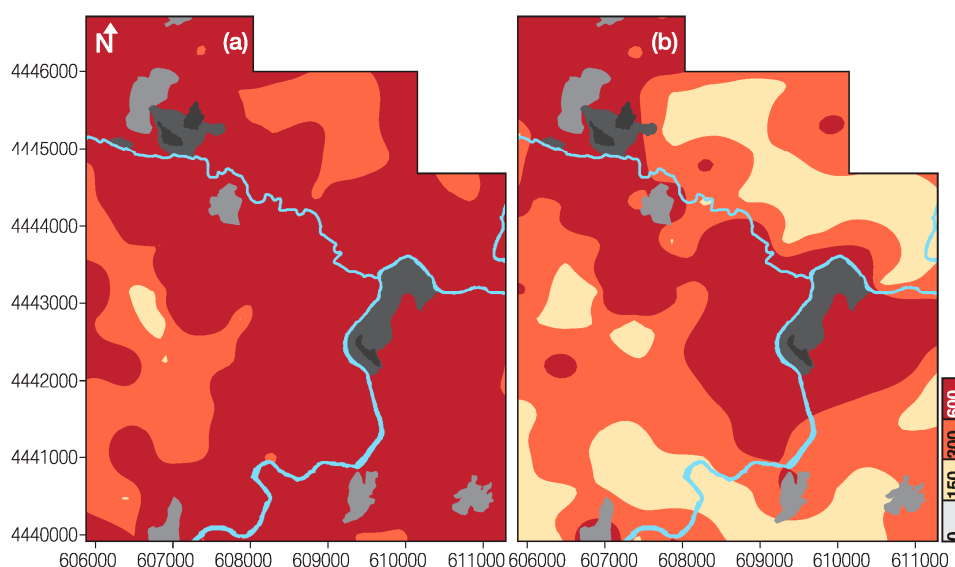
The topsoil and subsoil samples results for individual element potential pollution factor (EF) and potential ecological risk ($PERI$) are presented in Table 9. For both soil sample depths, As, Cu and Zn show a low potential ecological risk, with median values <40 (see Table 2). Tungsten also exhibits a low risk in subsoil, but a high risk in topsoil, while Bi and Ag show a moderate risk at both depths. Cadmium presents a very high ecological risk in topsoil and a high risk on subsoil. Using the median values, the topsoil risk factor is ranked as: $\text{Cd} > \text{W} > \text{Ag} > \text{Bi} > \text{As} \gg \text{Cu} > \text{Zn}$, while for subsoil the ranking is: $\text{Cd} > \text{Ag} > \text{Bi} > \text{As} > \text{Cu} = \text{W} > \text{Zn}$. These results suggest a very high environmental risk, especially for Cd.

In order to estimate the global potential ecological risk in the study area, the $PERI$ was computed. The median values classify soil samples at both depths with a very high risk (Table 9). The cumulative analysis shows that the soil samples at both depths do not display a low risk index (<150), and only 7.4% of topsoil present a moderate risk index. $PERI$ classified 92.6% of topsoil samples as high to very high ecological risk. The same occurs for 61.2% of subsoil samples, which should be considered as an extensive hazard. Figure 6 displays the $PERI$ spatial distribution. Topsoil has a wide area classified with a very high ecological risk, which is consistent with the wind direction, the water courses and the actual and previous exploration and beneficiation locations (Figure 6a). Subsoil also presents a very high risk index in the same topsoil areas, but with smaller area expression. These results are consistent with those mapped by the individual elements, Ag, As, Bi, Cd, Cu, W and Zn (Figures 2–4), and the modified degree of contamination (mC_d ; Figure 5), with the same affected areas.

Table 9. Statistical results of the single element potential pollution factor (*EF*) and potential ecological risk (*PERI*) for topsoil and subsoil samples.

Var	Ag _{EF}	As _{EF}	Bi _{EF}	Cd _{EF}	Cu _{EF}	W _{EF}	Zn _{EF}	PERI
Topsoil	Min	120	4	20	150	1	9	224
	Mean	120	23	127	893	3	573	1,740
	Med	70	15	60	600	2	255	1,020
	Max	1,190	338	4,300	9,000	21	8,571	23,353
Subsoil	Min	30	4	10	125	2	2	173
	Mean	76	33	56	418	7	8	600
	Med	60	23	30	250	6	6	350
	Max	360	158	770	3,750	26	203	4,369

Figure 6. Spatial distribution of Potential Ecological Risk Index (*PERI*) for topsoil (a) and subsoil (b) in the study area.

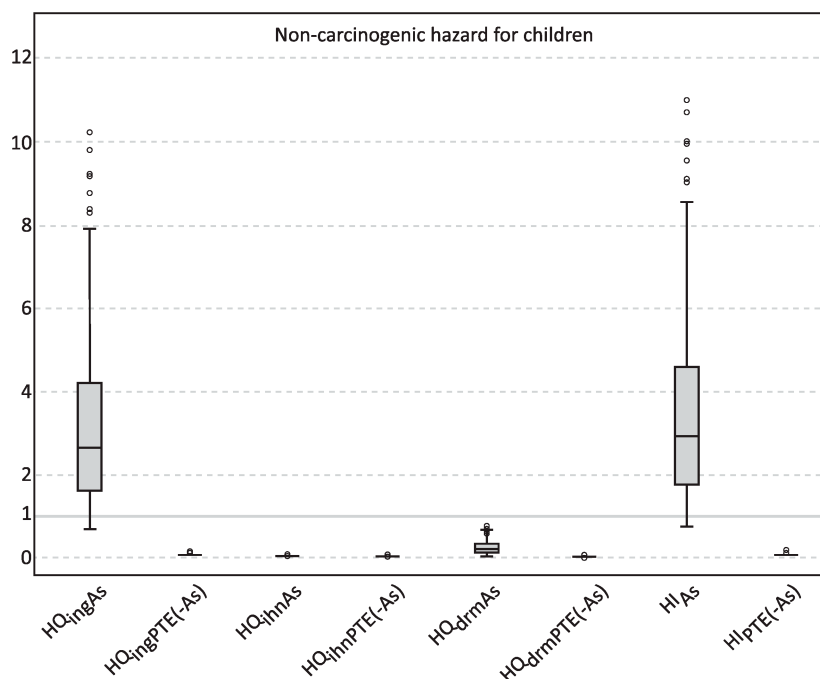


3.4. Human Health Risk Assessment

Both non-carcinogenic hazard (*HQ*) and carcinogenic risk (*Risk_{pathway}*) of topsoil in the Panasqueira mine and surrounding area, through the different pathways (ingestion, dermal and inhalation), were estimated according to the human health risk assessment model [28]. The cumulative hazard index (*HI*) and total risk (*Risk_{total}*) were also characterized for multi-pathway routes in resident population.

The non-carcinogenic effects considered the most conservative exposure condition—children (1–6 years old). The potentially toxic elements defined in this study (Ag, Cd, Cu, W and Zn), apart from As, do not present a non-carcinogenic hazard for children in the Panasqueira area (maximum $HI_{child-Ag,Cd,Cu,W,Zn} \leq 0.37$). The As non-carcinogenic hazard median values, estimated for the different exposure routes were $HQ_{ing-As} (2.75) \gg HQ_{drm-As} (0.23) \gg HQ_{inh-As} (0.00)$. $HI_{child-As}$ values ranged between 0.78 and 69.50, with a median value of $2.98 \approx HQ_{ing-As} (2.70)$, due to the ingestion hazard quotient ranging between 0.72 and 64.10. These results (<1—safe level) indicate that there is a cause for concern for the non-cancer health effects for children living in the Panasqueira study area, mainly due to As oral ingestion, with HQ_{ing-As} showing median values above one (Figure 7).

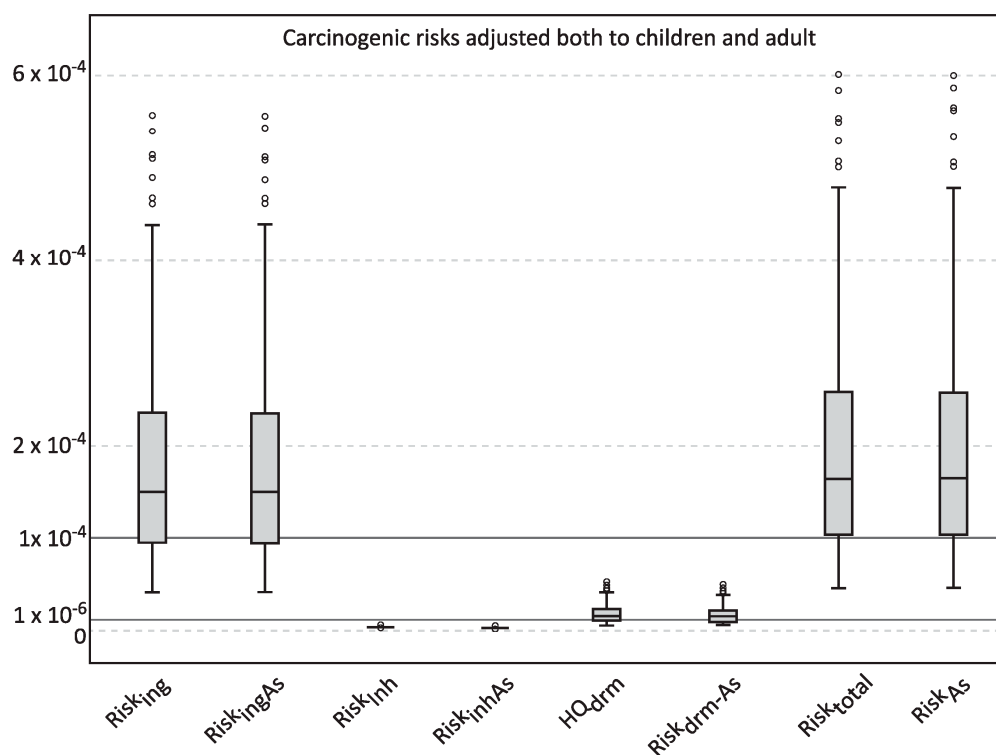
Figure 7. Comparative boxplot distribution of the Non-carcinogenic Hazard Quotient for children of As for Ingestion (HQ_{ingAs}), Inhalation (HQ_{inhAs}), Dermal contact (HQ_{drmAs}) routes, the Cumulative Hazard Index (HI_{As}) and the sum of the Non-carcinogenic Hazard Quotient of the other defined PTEs (Ag, Cd, Cu, W and Zn) for Ingestion ($HQ_{ingPTE(-As)}$), Inhalation ($HQ_{inhPTE(-As)}$), Dermal contact ($HQ_{drmPTE(-As)}$) routes and the Cumulative Hazard Index ($HI_{PTE(-As)}$) for topsoil samples (tailing samples were removed) in the Panasqueira area. The extremes and outliers were removed.



The carcinogenic risks adjusted both to children and adult were studied for the identified PTEs in this study. The median values of the different exposure routes and total risk were estimated. Their mean distribution were $Risk_{total}$ (2.62×10^{-4}) \approx $Risk_{As}$ (2.62×10^{-4}) \approx $Risk_{ing}$ (2.39×10^{-4}) \approx $Risk_{ingAs}$ (2.39×10^{-4}) \gg $Risk_{drm}$ (2.26×10^{-5}) \approx $Risk_{drmAs}$ (2.26×10^{-5}) \gg $Risk_{inh}$ (1.32×10^{-7}) \approx $Risk_{inhAs}$ (1.32×10^{-7}) (Figure 8). The high significance of As to cumulative carcinogenic elements risk is due to the very low risk displayed by the other elements. Furthermore, the representation of the exposure routes are distributed as: (a) $Risk_{ing} \approx Risk_{ingAs}$ ranged 3.97×10^{-5} – 3.53×10^{-3} , with a median value of 1.52×10^{-4} ; (b) $Risk_{drm} \approx Risk_{drmAs}$ ranged 3.76×10^{-6} – 3.34×10^{-4} , with median value of 1.44×10^{-5} ; and (c) $Risk_{inh} \approx Risk_{inhAs}$ ranged 2.21×10^{-8} – 1.96×10^{-6} , with median value of 8.38×10^{-8} . The cumulative pathway $Risk_{total} \approx Risk_{As}$ ranged 4.35×10^{-5} – 3.87×10^{-3} , with a median $Risk_{total}$ of 1.66×10^{-4} mostly due to $Risk_{ingAs}$. Intake of As may cause cancer in several human organs through ingestion, and lung and skin cancer through inhalation [28]. Moreover, the $Risk_{ing}$ represents 91.29% of cumulative risk from exposure routes, while $Risk_{drm}$ (8.69%) and $Risk_{inh}$ (0.05%) have less significance. Similar results were obtained in other studies [77,91–94]. The cumulative median $Risk_{drm}$ is $> 1 \times 10^{-6}$ for all samples, of which 69.67% $> 1 \times 10^{-5}$, and the cumulative exposure route median $Risk_{ing}$ is $> 1 \times 10^{-5}$ for all samples, being 72.13% $> 1 \times 10^{-4}$. These results show that there is a very high As ingestion cancer risk. The samples with higher hazard are located in and around the villages of the study area, being the more representative results found nearby the large tailing piles and open air

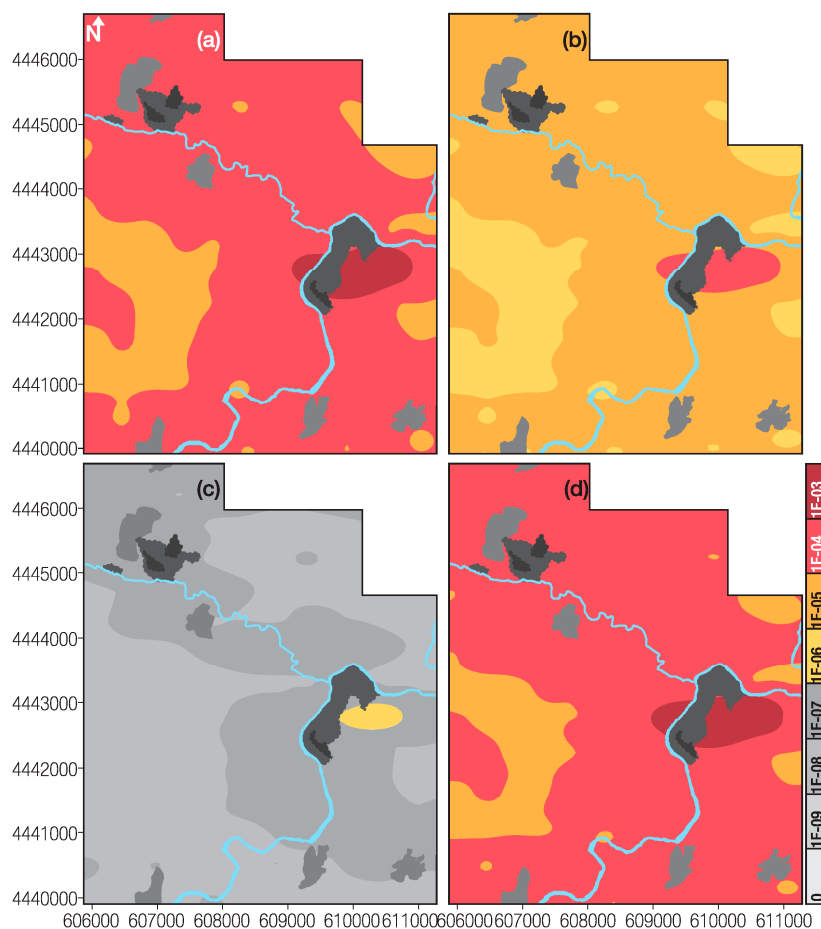
impoundments (Figure 9). Although the median $Risk_{drm}$ value is lower and between 1×10^{-6} and 1×10^{-4} , and is considered as acceptable, it cannot, however, be negligible in the Panasqueira mining area, once all samples exceed the target value (1×10^{-6}). While the sum of exposure pathways is $Risk_{Cd} = 1.09 \times 10^{-10}$ ($< 1 \times 10^{-6}$), it should be noted that it is the cumulative toxic metal and kidney index that is the main target for Cd toxicity [26,95].

Figure 8. Comparative boxplot distribution of the Carcinogenic Risk adjusted to both children and adult for total PTEs (Ag, As, Cd, Cu, W and Zn) for Ingestion ($Risk_{ing}$), Inhalation ($Risk_{inh}$), Dermal contact ($Risk_{drm}$) routes, the Cumulative Risk ($Risk_{total}$) and the Carcinogenic Risk of As for Ingestion ($Risk_{ingAs}$), Inhalation ($Risk_{inhAs}$), Dermal ($Risk_{drmAs}$) routes and the Cumulative Risk ($Risk_{As}$) for topsoil samples (tailing samples were removed) of the Panasqueira area. The extremes and outliers were removed.



As the risk analyses showed that ingestion is the most important pathway, further studies should be carried out in order to estimate the metal bioaccessibility in human receptors, such as a simplified *in vitro* physiologically based extraction test (PBET), allowing the estimation of the percentage of the bioaccessible orally ingested fraction of each metal from soil samples [77,80,96]. Additional investigations must be made on different sample media, such as vegetables, rhizosphere, irrigation and drinking water and street dust in the local villages under influence of mining activities (such as S. Francisco de Assis and Barroca) and also in non-exposed villages considered as reference areas (such as Casegas and Unhais-o-Velho). These studies will provide the necessary data and information for the determination of the influence of the Panasqueira mine activities, through more than 110 years, on the surrounding population, and should be complemented by biological studies [97].

Figure 9. Spatial distribution of the Carcinogenic risk adjusted for both children and adult considering (a) ingestion; (b) dermal contact; (c) inhalation routes; and (d) the cumulative Risk.



4. Conclusions

The mining and beneficiation process generates huge quantities of waste materials from the ore extraction and milling operations, which accumulate in tailings and open impoundments and are largely responsible for the high levels of metals(loid)s released into the surrounding environment. At the Panasqueira mine, the mining activities have produced sulphide-rich mine wastes that are responsible for the high levels of metals at Barroca Grande and Rio tailings. The oxidation of these sulphides may give rise to the mobilization and migration of trace metals from the mining wastes into the soil. Heavy metal soil contamination is an outstanding example of environmental risk. Metal(loid)s, such as As, Cd or Pb, for example, are toxic for humans, as well as for animals, and can even lead to death if ingested in large doses, or over large periods of time. Exposure to hazardous elements may have different pathways, such as ingestion, dermal absorption and inhalation of soil particles present in the air.

Collection of surface soil permits the characterization of anthropogenic contamination, caused by the presence of tailings and open air impoundments. Such soil, classified globally as very acid to acid, occurs in areas with very low soil pH values, which are related to areas with the highest SOM values. The metal assemblage identified in these soil types (Ag, As, Bi, Cd, Cu, W and Zn) show highest

values in topsoil samples (0–15 cm), when compared with the values of the corresponding subsoil samples below 15 cm depth. Soil samples from both depths have higher contents when compared to the estimated local geochemical background. These results show the influence of the metal-rich mine wastes, stored in Barroca Grande and Rio tailings and in the open impoundments, as the main source of pollution of the surrounding environment, possibly due to aerial transport and deposition.

Very strong correlations were estimated between the PTEs and between PTEs and pH. The strongest correlations were Ag/Cu, As/Ag and Bi/W. The PTEs and pH positive correlation, confirm the findings of other studies that heavy metal mobility holds a positive correlation with pH, affecting their availability.

The ANOVA results, showed significant variations with depth, and the majority of the PTEs (Ag, As, Bi, Cd and W) and pH exhibit a significant variation for Ag, W and Zn.

According to the calculated contamination factor (*CF*) and the modified degree of contamination (*mCa*), 7.4% of the soil samples were classified as having no to low degree of pollution with $mCa < 2.0$ and 92.6% registered moderate to ultra-high degree of pollution with $mCa \geq 2.0$. The spatial distribution of the *mCa* reveals areas with a very high degree of contamination. The highest *mCa* values were identified near Barroca Grande, São Francisco de Assis and Rio, and confirm the mechanical and chemical dispersion from tailings.

The risk factor estimated for individual element potential pollution factor and potential ecological risk, revealed at both soil sample depths that As, Cu and Zn have a low potential ecological risk, W low risk in subsoil, but a very high risk in topsoil samples; Ag moderate to considerable ecological risk and Cd is the worst element, exhibiting a very high environmental risk. The estimated potential ecological risk (*PERI*) classifies samples from both depths with a very high risk. In the *PERI* spatial distribution, topsoil has a wide area classified with a very high ecological risk, consistent with wind direction, water courses and current and previous exploration and beneficiation locations.

The non-carcinogenic hazard effects, determined for children (1–6 years old), indicated that the PTEs (Ag, Cd, Cu, W and Zn) do not present a non-carcinogenic hazard for children, while the As value is high, representing a risk for the non-cancer health effects for children in the Panasqueira area. The carcinogenic risk for both children and adults, revealed a very high cancer risk due to As ingestion, which may cause cancer to several human organs cancer through ingestion, and lung and skin cancer through inhalation.

Further studies should be carried out in order to estimate the metal bioaccessibility in human receptors.

Acknowledgments

This research is financially supported by FCT—Fundação para a Ciência e a Tecnologia (grants SFRH/BD/63349/2009).

Author Contributions

The original idea of the study was designed on a brainstorm meeting by all authors. E. Ferreira da Silva and J. P. Teixeira were responsible for recruitment and follow-up of study participants. All authors participated on the field work. C. Candeias and P. F. Ávila were responsible for data cleaning and

analyses. C. Candeias drafted the manuscript with collaboration of all authors and it was revised by all. All authors read and approved the final manuscript.

Conflicts of Interest

The authors declare no conflict of interests.

References

1. Cohen, R.R.H.; Gorman, J. Mining-related nonpoint-source pollution. *Water Environ. Technol.* **1991**, *3*, 55–59.
2. Merson, J. Mining with microbes. *N. Sci.* **1992**, *133*, 9–17.
3. Evangelou, V.P.B.; Zhang, Y.L. A review: Pyrite oxidation mechanisms and acid mine drainage prevention. *Crit. Rev. Environ. Sci. Technol.* **1995**, *25*, 141–199.
4. Larocque, A.C.L.; Rasmussen, P.E. An overview of trace metals in the environment, from mobilization to remediation. *Environ. Geol.* **1998**, *33*, 85–91.
5. Soucek, D.J.; Cherry, D.S.; Currie, R.J. Laboratory to field validation in an integrative assessment of an acid mine drainage-impacted watershed. *Environ. Toxicol. Chem.* **2000**, *19*, 1036–1043.
6. Candeias, C. Modelling the Impact of Panasqueira Mine in the Ecosystems and Human Health: A Multidisciplinary Approach. Ph.D. Thesis, Aveiro University/Porto University, Aveiro, Portugal, 2013.
7. Rasmussen, P.E. Long-range atmospheric transport of trace metals: The need for geosciences perspectives. *Environ. Geol.* **1998**, *33*, 96–108.
8. Yukselen, M.A.; Alpaslan, B. Leaching of metals from soil contaminated by mining activities. *J. Hazard Mater.* **2001**, *87*, 289–300.
9. Chen, X.; Wright, J.V.; Conca, J.L.; Peurrung, L.M. Evaluation of heavy metal remediation using mineral apatite. *Water Air Soil Pollut.* **1997**, *98*, 57–78.
10. Bosso, S.T.; Enzweiler, J. Bioaccessible lead in soils, slag, and mine wastes from an abandoned mining district in Brazil. *Environ. Geochem. Health* **2008**, *30*, 219–229.
11. Douay, F.; Pruvot, C.; Roussel, H.; Ciesielski, H.; Fourrier, H.; Proix, N.; Waterlot, C. Contamination of urban soils in an area of Northern France polluted by dust emissions of two smelters. *Water Air Soil Pollut.* **2008**, *188*, 247–260.
12. Roussel, H.; Waterlot, C.; Pelfrêne, A.; Pruvot, C.; Mazzuca, M.; Douay, F. Cd, Pb and Zn Oral Bioaccessibility of urban soils contaminated in the past by atmospheric emissions from two lead and zinc smelters. *Arch. Environ. Contam. Toxicol.* **2010**, *58*, 945–954.
13. Juhasz, A.L.; Weber, J.; Smith, E. Impact of soil particle size and bioaccessibility on children and adult lead. *J. Hazard Mater.* **2011**, *186*, 1870–1879.
14. Ettler, V.; Kribek, B.; Majer, V.; Knesl, I.; Mihaljevic, I. Differences in the bioaccessibility of metals/metalloids in soils from mining smelting areas (Copperbelt, Zambia). *J. Geochem. Explor.* **2012**, *113*, 68–75.
15. Banza, C.L.N.; Nawrot, T.S.; Haufroid, V.; Decre, S.; de Putter, T.; Smolders, E.; Kabyala, B.I.; Luboya, O.N.; Ilunga, A.N.; Mutombo, A.M.; *et al.* High human exposure to cobalt and other metals in Katanga, a mining area of the Democratic Republic of Congo. *Environ. Res.* **2009**, *109*, 745–752.

16. Radojevic, M.; Bashki, V.N. *Practical Environmental Analysis*; The Royal Society of Chemistry: Cambridge, UK, 2006.
17. Krishnamurti, G.S.R.; Huang, P.M.; Kozak, L.M. Sorption and desorption kinetics of cadmium from soils: Influence of phosphate. *Soil Sci.* **1999**, *164*, 888–898.
18. Antoniadis, V.; Robinson, J.S.; Alloway, B.J. Effects of short-term pH fluctuations on cadmium, nickel, lead, and zinc availability to ryegrass in a sewage sludge-amended field. *Chemosphere* **2008**, *71*, 759–764.
19. Mühlbachová, G.; Simon, T.; Pechová, M. The availability of Cd, Pb and Zn and their relationships with soil pH and microbial biomass in soils amended by natural clinoptilolite. *Plant Soil Environ.* **2005**, *51*, 26–33.
20. Zhao, K.L.; Liu, X.M.; Xu, J.M.; Selim, H.M. Heavy metal contaminations in a soil-rice system: Identification of spatial dependence in relation to soil properties of paddy fields. *J. Hazard Mater.* **2010**, *181*, 778–787.
21. Zeng, F.; Ali, S.; Zhang, H.; Ouyang, Y.; Qiu, B.; Wu, F.; Zhang, G. The influence of pH and organic matter content in paddy soil on heavy metal availability and their uptake by rice plants. *Environ. Pollut.* **2011**, *159*, 84–91.
22. Sukreeyapongse, O.; Holme, P.E.; Strobel, B.W.; Panichsakpatana, S.; Magid, J.; Hansen, H.C.B. pH-dependent release of cadmium, copper, and lead from natural and sludge-amended soils. *J. Environ. Qual.* **2002**, *31*, 1901–1909.
23. Oliver, D.P.; Tiller, K.G.; Connyers, M.K.; Sattery, W.J.; Alston, A.M.; Merry, R.H. Effectiveness of liming to minimise uptake of cadmium by wheat and barley grain grown in the field. *Aust. J. Agric. Res.* **1996**, *47*, 1181–1193.
24. Braillier, S.; Harrison, R.B.; Henry, C.L.; Dogsen, X. Liming effects on availability of Cd, Cu, Ni and Zn in a soil amended with sewage sludge 16 years previously. *Water Air Soil Pollut.* **2006**, *86*, 195–206.
25. Du Laing, G.; Vanthuyne, D.R.J.; Vandecasteele, B.; Tack, F.M.G.; Verloo, M.G. Influence of hydrological regime on pore water metal concentrations in a contaminated sediment-derived soil. *Environ. Pollut.* **2007**, *147*, 615–625.
26. Zheng, N.; Liu, J.; Wang, Q.; Liang, Z. Health risk assessment of heavy metal exposure to street dust in the zinc smelting district, Northeast of China. *Sci. Total Environ.* **2010**, *408*, 726–733.
27. Mudgal, V.; Madaan, N.; Mudgal, A.; Singh, R.B.; Mishra, S. Effect of toxic metals on human health. *Open Nutraceuticals J.* **2010**, *3*, 94–99.
28. U.S. Department of Energy. *The Risk Assessment Information System (RAIS)*; U.S. Department of Energy's Oak Ridge Operations Office (ORO): Oak Ridge, TN, USA, 2013.
29. Agency for Toxic Substances and Disease Registry. Available online: <http://www.atsdr.cdc.gov/> (accessed on 23 September 2014).
30. World Health Organization (WHO). Monographs-Analytical and Toxicological Data. In *Basic Analytical Toxicology*; World Health Organization: Geneva, Switzerland, 2013.
31. *National Drug Formulary of Ethiopia*; Drug Administration and Control Authority of Ethiopia (DACAE): Addis Ababa, Ethiopia, 2007.

32. Candeias, C.; Ferreira da Silva, E.; Ávila, P.F.; Salgueiro, A.R.; Teixeira, J.P. Integrated approach to assess the environmental impact of mining activities: Multivariate statistical analysis to estimate the spatial distribution of soil contamination in the Panasqueira mining area (Central Portugal). *Environ. Monit. Assess.* **2014**, in press.
33. Smith, M. Panasqueira the tungsten giant at 100+. *Oper. Focus. Int. Min.* **2006**, *33*, 10–14.
34. Thadeu, D. Geologia do couto mineiro da Panasqueira. *Comunicações dos Serviços Geológicos de Portugal* **1951**, *32*, 5–64. (In Portuguese)
35. Bloot, C.; de Wolf, L.C.M. Geological features of the Panasqueira tin-tungsten ore occurrence (Portugal). *Bol. Soc. Geol. Port.* **1953**, *11*, 1–58.
36. Kelly, W.C.; Rye, R.O. Geologic, fluid inclusion and stable isotope studies of the tin-tungsten deposits of Panasqueira, Portugal. *Econ. Geol.* **1979**, *74*, 1721–1822.
37. Polya, D.A. Chemistry of the main stage ore-forming fluids of the Panasqueira W-Cu(Ag)-Sn deposit, Portugal: Implications for models of ore genesis. *Econ. Geol.* **1989**, *84*, 1134–1152.
38. Noronha, F.; Dória, A.; Dubessy, J.; Charoy, B. Characterisation and timing of the different types of fluids present in the barren and ore-veins of the W-Sn deposit of Panasqueira, Central Portugal. *Miner. Deposita* **1992**, *27*, 72–79.
39. Correia, A.; Naique, R.A. Minas Panasqueira, 100 Years of Mining History. In Proceedings of the International Tungsten Industrial Association (ITIA) Conference, Salzburg, Austria, 20–22 October 1998.
40. Corrêa de Sá, A.; Naique, R.A.; Nobre, E. Minas da Panasqueira: 100 anos de História. *Bol. Minas* **1999**, *36*, 3–22. (In Portuguese)
41. *e-Ecorisk, A Regional Enterprise Network Decision-Support System for Environmental Risk and Disaster Management of Large-Scale Industrial Soils, Contract n.º EGV1-CT-2002-00068; WP3—Case Study Site Characterization, Project Management Report for the Reporting Period, Deliverable 3.1; Joanneum Research Forschungsgesellschaft—GMBH: Frohnleiten, Austria, 2007; not published.*
42. Ávila, P.; Ferreira da Silva, E.; Salgueiro, A.; Farinha, J.A. Geochemistry and Mineralogy of Mill Tailings Impoundments from the Panasqueira Mine (Portugal): Implications for the Surrounding Environment. *Mine Water Environ.* **2008**, *27*, 210–224.
43. Ferreira da Silva, E.; Ávila, P.F.; Salgueiro, A.R.; Candeias, C.; Pereira, H.G. Quantitative–spatial assessment of soil contamination in S. Francisco de Assis due to mining activity of the Panasqueira mine (Portugal). *Environ. Sci. Pollut. Res.* **2013**, *20*, 7534–7549.
44. Candeias, C.; Melo, R.; Ávila, P.F.; Ferreira da Silva, E.; Salgueiro, A.R.; Teixeira, J.P. Heavy metal pollution in mine–soil–plant system in S. Francisco de Assis–Panasqueira mine (Portugal). *Appl. Geochem.* **2014**, *44*, 12–26.
45. Jaques Ribeiro, L.M.; Gonçalves, A.C.R. Contributo para o conhecimento geológico e geomorfológico da área envolvente do Couto Mineiro da Panasqueira. Centro de Estudos de Geografia e Ordenamento do Território. *Revista de Geografia e Ordenamento do Território* **2013**, *3*, 93–116. (In Portuguese)
46. *Atlas do Potencial Eólico para Portugal Continental, Version 1.0 [CD-ROM]; ISBN 972-676-196-4; Instituto Nacional de Engenharia, Tecnologia e Inovação I.P. (INETI): Lisboa, Portugal, 2004. (In Portuguese)*

47. Reis, A.C. As Minas da Panasqueira. *Bol. Minas* **1971**, *8*, 3–34. (In Portuguese)
48. Costa, P.; Estanqueiro, A. Development and Validation of the Portuguese Wind Atlas. In Proceedings of the European Wind Energy Conference, Athens, Greece, 27 February–2 March 2006.
49. Costa, P.; Estanqueiro, A. Building a Wind Atlas for Mainland Portugal Using a Weather Type Classification. In Proceedings of the European Wind Energy Conference, Athens, Greece, 27 February–2 March 2006.
50. Costa, P.A.S. Atlas do Potencial eólico para Portugal Continental. Master's Thesis, University of Lisbon, Lisboa, Portugal, 2004. (In Portuguese)
51. Turner, A.P. The responses of plants to heavy metals. In *Toxic Metals in Soil-Plant Systems*; Sheila, M.R., Ed.; John Wiley & Sons: Hoboken, NJ, USA, 1994.
52. McBride, M.B.; Richards, B.; Steenhuis, T.; Russo, J.J.; Sauvé, S. Mobility and solubility of toxic metals and nutrients in soil fifteen years after sludge application. *Soil Sci.* **1997**, *162*, 487–500.
53. Van Reeuwijk, L.P. *Procedures for Soil Analysis*, 6th ed.; International Soil Reference and Information Centre: Wageningen, The Netherlands, 2002.
54. ISO 10390:1994 Soil; In *Soil Quality—Determination of pH*; International Organization for Standardization: Geneva, Switzerland, 1995.
55. Schnitzer, M.; Khan, S.U. *Substances in the Environment*; Marcel Dekker: New York, NY, USA, 1972.
56. Stevenson, F.J. *Humus Chemistry*; Wiley: New York, NY, USA, 1982.
57. Yin, Y.; Allen, H.E.; Huang, C.P.; Sparks, D.L.; Sanders, P.F. Kinetics of mercury (II): Adsorption and desorption on soil. *Environ. Sci. Technol.* **1997**, *31*, 496–503.
58. You, S.J.; Yin, Y.; Allen, H.E. Partitioning of organic matter in soils: Effects of pH and water soil ratio. *Sci. Total Environ.* **1999**, *227*, 155–160.
59. Zar, J.H. *Biostatistical Analysis*; Prentice Hall: New York, NY, USA, 1996.
60. Johnson, R.A.; Wichern, D.W. *Applied Multivariate Statistical Analysis*; Prentice-Hall: New York, NY, USA, 1998.
61. Corwin, D.L.; Lesh, S.M.; Oster, J.D.; Kaffka, S.R. Monitoring management-induced spatio-temporal changes in soil quality through soil sampling direct by apparent electrical conductivity. *Geoderma* **2006**, *131*, 369–387.
62. Hakanson, L. Ecological risk index for aquatic pollution control, a sedimentological approach. *Water Res.* **1980**, *14*, 975–1001.
63. Loska, K.; Wiechula, D.; Korus, I. Metal contamination of farming soils affected by industry. *Environ. Int.* **2004**, *30*, 159–165.
64. Liu, W.H.; Zhao, J.Z.; Ouyang, Z.Y.; Solderland, L.; Liu, G.H. Impacts of sewage irrigation on heavy metal distribution and contamination in Beijing, China. *Environ. Int.* **2005**, *32*, 805–812.
65. Tuckey, J.W. *Exploratory Data Analysis*; Addison Wesley: Boston, MA, USA, 1977.
66. Abraham, G.M.S.; Parker, R.J. Assessment of heavy metal enrichment factors and the degree of contamination in marine sediments from Tamaki Estuary, Auckland, New Zealand. *Environ. Monit. Assess.* **2008**, *136*, 227–238.
67. Reimann, C.; Caritat, P. *Chemical Elements in the Environment: Factsheets for the Geochemist and Environmental Scientist*; Springer: Berlin, Germany, 1998.
68. Bowen, H.J.M. *Trace Elements in Biochemistry*; Academic Press: London, UK, 1966.

69. U.S. Environmental Protection Agency (USEPA). *Risk Assessment Guidance for Superfund, Volume I: Human Health Evaluation Manual*; EPA 540-1-89-002; U.S. Environmental Protection Agency: Washington, DC, USA, 1989.
70. U.S. Environmental Protection Agency (USEPA). *Soil Screening Guidance: Technical Background Document*; EPA 540-R-95-128; U.S. Environmental Protection Agency: Washington, DC, USA, 1996.
71. Linders, J.B.H.J. Risicobeoordelino voor de mens bij blootstelling aan stoffen: Uitgangspunten en veronderstellingen. In *Rapport/Rijksinstituut voor Volksgezondheid en Milieuhygiene (nr. 725201003)*; RIVM: Bilthoven, The Netherlands, 1990. (In Dutch)
72. Berg, R.V.D. *Human Exposure to Soil Contamination: A Qualitative and Quantitative Analysis towards Proposals for Human Toxicological Intervention Values (Partly Revised Edition)*; Report No. 725201011; National Institute for Public Health and the Environment: Bilthoven, The Netherlands, 1994.
73. U.S. Environmental Protection Agency (USEPA). *Risk Assessment Guidance for Superfund: Volume III—Part A, Process for Conducting Probabilistic Risk Assessment*; EPA 540-R-02-002; U.S. Environmental Protection Agency: Washington, DC, USA, 2001.
74. U.S. Environmental Protection Agency (USEPA). *Integrated Risk Information System (IRIS)*; U.S. Environmental Protection Agency: Washington, DC, USA, 2013.
75. INE. Portal do Instituto Nacional de Estatística—Statistics Portugal. Available online: <http://www.ine.pt/> (accessed on 23 September 2014). (In Portuguese)
76. U.S. Environmental Protection Agency (USEPA). *Guidance for Evaluating the Oral Bioavailability of Metals in Soils for Use in Human Health Risk Assessment*; OSWER 9285.7-80; U.S. Environmental Protection Agency: Washington, DC, USA, 2007.
77. Luo, X.S.; Ding, J.; Xu, B.; Wang, Y.J.; Li, H.B.; Yu, S. Incorporating bioaccessibility into human health risk assessments of heavy metals in urban park soils. *Sci. Total Environ.* **2012**, *424*, 88–96.
78. Hu, X.; Zhang, Y.; Luo, J.; Wang, T.; Lian, H.; Ding, Z. Bioaccessibility and health risk of arsenic, mercury and other metals in urban street dusts from a mega-city, Nanjing, China. *Environ. Pollut.* **2011**, *159*, 1215–1221.
79. U.S. Environmental Protection Agency (USEPA). *Screening Levels (RSL) for Chemical Contaminants at Superfund Sites*; U.S. Environmental Protection Agency: Washington, DC, USA, 2013.
80. Luo, X.S.; Yu, S.; Li, X.D. The mobility, bioavailability, and human bioaccessibility of trace metals in urban soils of Hong Kong. *Appl. Geochem.* **2012**, *27*, 995–1004.
81. U.S. Department of Agriculture. Available online: <http://www.nrcs.usda.gov> (accessed on 23 September 2014).
82. Tidball, R.R.; Ebens, R.J. Regional geochemical baselines in soils of the Powder River Basin, Montana–Wyoming. In *Geology and Energy Resources of the Powder River*; 28th Annual Field Conference Guidebook; American Association of Petroleum Geologists (AAPG): Tulsa, OK, USA, 1976.
83. Ministry of the Environment. *Soil, Ground Water and Sediment Standards for the Use under Part XV.1 of the Environmental Protection Act*; Ministry of the Environment: Ottawa, Canada, 2011.

84. Fiedler, H.J.; Rösler, H.J. *Spurenelemente in der Umwelt*; Gustav Fischer Verlag: Jena, Germany, 2013. (In German)
85. Mench, M. Notions sur les éléments en traces pour une qualité des sols et des produits végétaux. *Purpan* **1993**, *166*, 118–127. (In French)
86. Deschamps, E.; Ciminelli, V.S.T.; Lange, F.T.; Matschullat, J.; Raue, B.; Schmidt, H. Soil and sediment geochemistry of the iron quadrangle, Brazil: The case of arsenic. *J. Soils Sediment.* **2002**, *2*, 216–222.
87. Ferreira, M.M.S.I. Dados Geoquímicos de Base de Solos de Portugal Continental, Utilizando Amostragem de Baixa Densidade. Ph.D. Thesis, University of Aveiro, Aveiro, Portugal, 2004. (In Portuguese)
88. Yuan, G.; Lavkulich, L.M. Sorption behavior of copper, zinc, and cadmium in response to simulated changes in soil properties. *Commun. Soil Sci. Plant Anal.* **1997**, *28*, 571–587.
89. Hettiarachchi, G.M.; Ryan, J.A.; Chaney, R.L.; La Fleur, C.M. Sorption and desorption of cadmium by different fractions of biosolids-amended soils. *J. Environ. Qual.* **2003**, *32*, 1684–1693.
90. Qishlaqi, A.; Moore, F. Statistical analysis of accumulation and sources of heavy metals occurrence in agricultural soils of Khoshk River Banks, Shiraz, Iran. *J. Agric. Environ. Sci.* **2007**, *2*, 565–573.
91. Chabukdhara, M.; Nema, A.K. Heavy metals assessment in urban soil around insutrial clusters in Ghaziabad, India: Probabilistic health risk approach. *Ecotoxicol. Environ. Saf.* **2013**, *87*, 57–64.
92. De Miguel, E.; Iribarren, I.; Chacón, E.; Ordoñez, A.; Charlesworth, S. Risk-based evaluation of the exposure of children to trace elements in playgrounds in Madrid (Spain). *Chemosphere* **2007**, *66*, 505–513.
93. Ferreira-Baptista, L.; de Miguel, E. Geochemistry and risk assessment of street dust in Luanda, Angola: A tropical urban environment. *Atmos. Environ.* **2005**, *39*, 4501–4512.
94. Dudka, S.; Miller, W.P. Permissible concentrations of arsenic and lead in soils based on risk assessment. *Water Air Soil Pollut.* **1999**, *113*, 127–132.
95. De Burbure, C.; Buchet, J.P.; Bernard, A.; Leroyer, A.; Nisse, C.; Haguenoer, J.M.; Bergamaschi, E.; Mutti, A. Biomarkers of renal effects in children and adults with low environmental exposure to heavy metals. *J. Toxicol. Environ. Health* **2003**, *66*, 783–798.
96. Drexler, J.W.; Brattin, W.J. An *in vitro* procedure for estimation of lead relative bioavailability: With validation. *Hum. Ecol. Risk Assess.* **2007**, *13*, 383–401.
97. Coelho, P.; Costa, S.; Costa, C.; Silva, S.; Walter, A.; Ranville, J.; Pastorinho, R.; Harrington, C.; Taylor, A.; Dall’Armi, V.; *et al.* Biomonitoring of several toxic metal(loid)s in different biological matrices from environmentally and occupationally exposed populations from Panasqueira mine area, Portugal. *Environ. Geochem. Health* **2013**, *36*, 255–269.